

Baryonic Matter at Supercluster Scales: the case of the Corona Borealis Supercluster

Carmen Pilar Padilla-Torres¹, Rafael Rebolo^{1,2}, Carlos M. Gutiérrez¹, Ricardo Génova-Santos¹, José Alberto Rubiño-Martín¹

Abstract In a 24 deg² survey for baryonic matter at 33 GHz in the Corona Borealis supercluster (CrB-SC) of galaxies ($z=0.07$), with the Very Small Array (VSA) interferometer ([1],[2]), we found a very strong temperature decrement in the Cosmic Microwave Background (CMB). It has an amplitude of $-230 \pm 23 \mu\text{K}$ and is located near the centre of the supercluster, in a position with no known galaxy clusters, and without a significant X-ray emission in the *ROSAT* All-Sky Survey. Monte-Carlo simulations discard the primordial CMB Gaussian field as a possible explanation for this decrement at a level of 99.6%. We therefore concluded that this could be indicative of a Sunyaev-Zel'dovich (SZ) effect produced either by a warm/hot gas distribution in the intercluster medium or by a farther unknown galaxy cluster.

Here we present an optical study of the galaxy distribution in this region, aiming at elucidating whether it traces a possible warm/hot gas filamentary distribution or a galaxy cluster. First, we have studied the galaxy population down to $r \leq 20$ magnitudes in the SDSS. This reveals an overdensity by a factor of 2 with respect to nearby control fields, but lower than in the galaxy clusters member of the CrB-SC. This indicates that the associated gas could at least be partially responsible for the observed CMB decrement. Second, we obtained spectroscopic redshifts, with the William Herschel Telescope (WHT), for a sample of galaxies in the region of the cold spot, and found evidence of a substructure with redshifts extending from 0.07 to 0.10. This suggests the existence of a dense filamentary structure with a length of several tens of Mpc. Finally, we investigated the presence of at least one farther cluster in the same line-of-sight, at $z \approx 0.11$.

1 Introduction

Hydrodynamical simulations of the Large Scale Structure in the Universe indicate that a significant fraction of the baryonic matter is distributed in diffuse intergalactic structures of warm/hot gas within superclusters, with temperatures $10^5 \leq T \leq 10^7$ K.

¹Instituto de Astrofísica de Canarias, Spain cppt@iac.es

²Consejo Superior de Investigaciones Científicas, Spain rrl@iac.es

The CrB-SC is one of the most prominent examples of superclustering in the northern sky. Counts of galaxies in the Lick Observatory photographic plates were the first to show the extraordinary cloud of galaxies that constitute this supercluster [3]. This concentration of clusters of galaxies was later included in a catalogue of “second-order clusters” [4]. Depending on the author, the number of clusters belonging to this supercluster ranges from six to eight ([5],[6]). Here we will adopt the classification given by [7], which states the presence of eight clusters located around the coordinates R.A. = $15^{\text{h}}25^{\text{m}}16.2^{\text{s}}$, Dec. = $+29^{\circ}31'30''$, at a redshift $z \sim 0.07$. These clusters (A2061, A2065, A2067, A2079, A2089 and A2092) are located in a $\sim 3^{\circ} \times 3^{\circ}$ region in the core of the SC, while other two (A2019 and A2124) are located at an angular distance of $\sim 2.5^{\circ}$ from the core. Only A2061 and A2065 are X-ray emitting clusters [7]. There are other four Abell clusters (A2056, A2005, A2022 and A2122) in this region at $z \sim 0.07$, two (A2069 and A2083) at $z \sim 0.11$ and other two (A2059 and A2073) even more distant. The spatial distribution of these clusters can be seen in Fig. 1, that shows the density of galaxies with magnitudes $r \leq 22.2$ on the CrB-SC. An error restriction criterion in the principal photometric bands g, r and i has been applied.

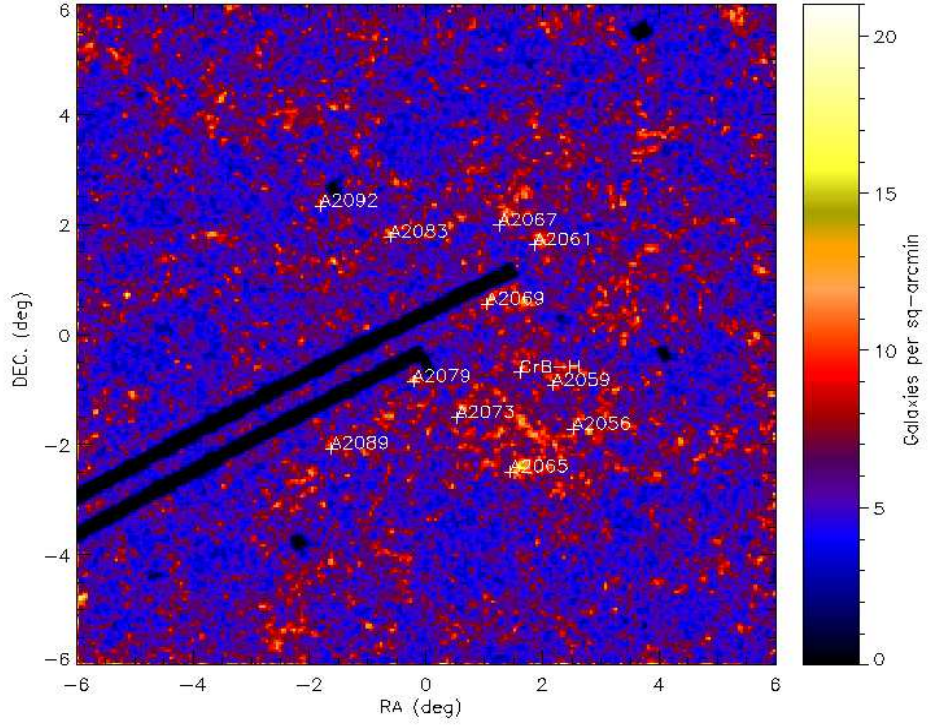


Fig. 1 SDSS-DR6 map of the density of galaxies in the CrB-SC region, built from the galaxy catalogue. Labels indicate the positions of the CMB decrement CrB-H and of the known Abell clusters.

The first dynamical study of the CrB-SC, based on a sample of 1555 galaxies [5], concluded that the masses of all clusters in the core lie in the range $1.5 - 8.9 \times 10^{14} M_{\odot}$, being the mass of the SC $\approx 8.2 \times 10^{15} M_{\odot}$, which is probably

enough to bind the system. A higher mass of $3 - 8 \times 10^{16} h^{-1} M_{\odot}$ has also been proposed [8]. Almost one third of the galaxies in the region are not linked to any Abell cluster. It is also emphasized the great contribution to the projected galaxy surface density of the background cluster A2069 and its surrounding galaxies, located at a redshift $z \sim 0.11$.

2 Supercluster studies

2.1 The VSA and MITO observations

The Corona Borealis Supercluster was observed at a frequency of ~ 33 GHz with the VSA, a CMB interferometer located at the *Observatorio del Teide*, using two different setups of antennas providing spatial resolutions of 11 and 7 arcmin respectively ([1],[2]). We found a large and very deep decrement in the CMB, named “CrB-H”, with a minimum temperature of $-230 \pm 23 \mu\text{K}$ and angular size ~ 20 arcmin, located at $15^{\text{h}}22^{\text{m}}11.47^{\text{s}}, +29^{\circ}00'02.6''$ (its position is shown in Fig. 1). No other similar spots have been found in any of the VSA primordial CMB observations [9], which shows that this is indeed a very particular feature in the CMB. Additional millimetric observations performed with the MITO telescope at 143, 214 and 272 GHz confirmed the presence of this decrement, and showed a spectrum compatible with an SZ effect [10].

An SZ effect in this region would be indicative of a large concentration of baryonic matter. This matter would be in the form of plasma at a temperature of several hundred thousand to about ten million degrees in a region where no clusters of galaxies have been identified. We should expect a galaxy population associated to such plasma, as it is well known to occur in clusters of galaxies where the SZ has been measured (see, e.g. [11]). However, the lack of any identified cluster and the absence of X-ray emission in the ROSAT images suggest that if there is a galaxy population linked to the plasma it may have peculiar spatial distribution and characteristics.

2.2 The SDSS-based photometric analysis and results

Using the *SDSS RS6 Catalogue Archive Server* we have produced a new photometric catalogue of CrB-SC galaxies. We note that in our data analysis we only used objects catalogued as galaxies by the SDSS algorithms, and we made a second restriction consisting of excluding objects with high photometric errors in the g, r and i bands. The final SDSS catalogue provides 121,235 galaxies under this selection criterion in the supercluster region. The map of galaxy density fluctuations shows a lack of galaxies in the region of the decrement as compared with the adjacent regions where the galaxy clusters are located (see Fig. 1). We carried out a test to es-

timate the expected background counts of galaxies in 1000 random zones of the sky by counting galaxies up to $r \leq 19$ mag. The density of galaxies within the CrB-H decrement is ~ 2 times higher than the mean value. We only found about $\sim 1 - 2\%$ of such random regions with larger galaxy densities than in the spot (see Fig. 2).

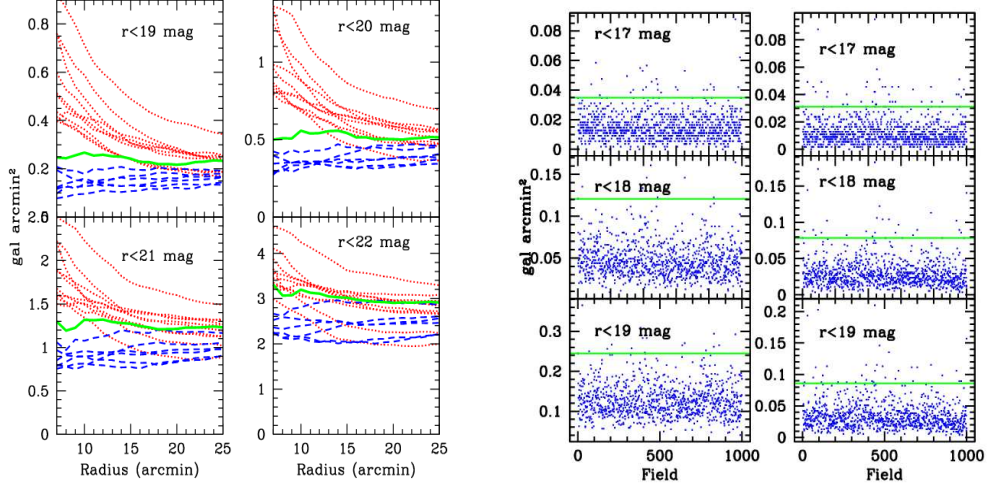


Fig. 2 Left: Density of galaxies as a function of the radius at the positions of: the CrB-H cold spot (solid line), clusters of galaxies within the CrB-SC (red dotted lines), and several intercluster regions (dashed lines). **Right:** Density of galaxies, from the SDSS-DR6 and after applying different cuts in r magnitude, in randomly selected areas (dots). The solid line represents the density of the corresponding galaxies within the CrB-H cold spot.

2.3 Spectroscopic analysis and results

By means of the AF2/WYFFOS multi-object, wide-field, fibre fed spectrograph on the WHT at the Roque de Los Muchachos Observatory, we have obtained spectroscopic redshifts for a sample of galaxies detected by the SDSS in the area of CrB-H with magnitudes in the range $r=16.0-18.5$, and for a sample of galaxies in A2065. Three campaigns have been conducted from 2006. In the first one we used the lower resolution $R158R$ grating, with a nominal dispersion of $\sim 5.8 \text{ \AA/pix}$. The spectral coverage provides emission Balmer lines, OII, OIII or SII and absorption lines such as CaII H and K, H_β , H_γ , MgI and the Balmer break. 71 redshifts were determined in such way. In the second and third campaigns we used the $R300B$ grating, which provides a nominal dispersion of $\sim 3.2 \text{ \AA/pix}$ and a spectral coverage of $\sim 4000 \text{ \AA}$.

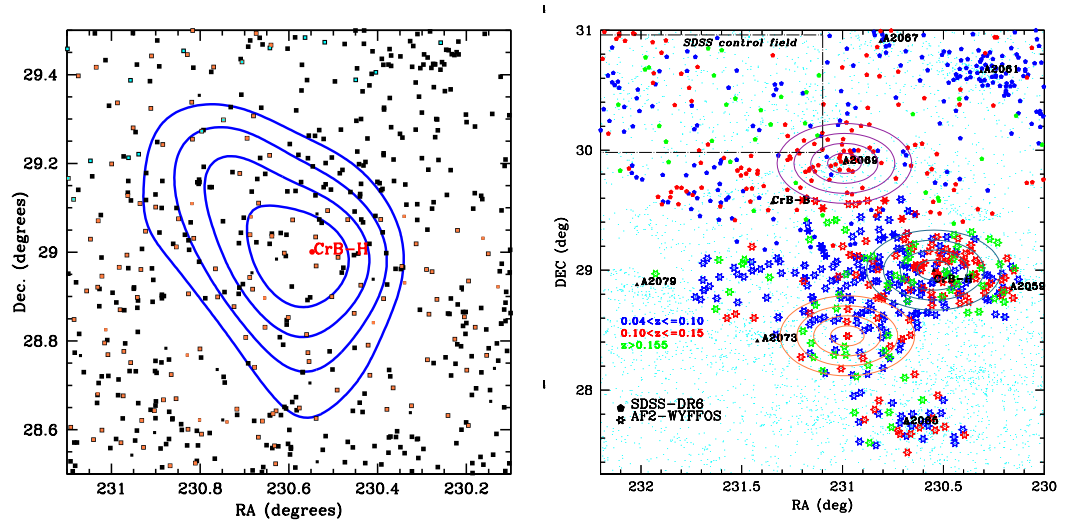


Fig. 3 Left: The SDSS spectroscopic survey and the AF2/WYFFOS survey. Galaxies with redshift determination in the SDSS-DR6 are shown in cyan; orange dots represent a sample of AF2-WYFFOS galaxies. We show galaxies observed with the last fiber configurations in black. Blue lines represent the 2, 3, 4 and 5 σ contours of the VSA map. **Right:** Galaxy distribution in the CrB-SC region. Pentagons represent galaxies with SDSS-DR6 spectroscopy, whereas stars show the galaxies for which spectroscopic redshifts have been obtained with AF2-WYFFOS. The large circles show the CrB-SC regions used to compare the CrB-H spot region, with A2069 at $z \approx 0.11$ and a control region out of the CrB-H spot.

We determined the redshifts of 212 and 117 galaxies, with magnitudes $r \leq 18.5$ and up to $r \leq 19.5$ respectively. Data reduction was done with IRAF packages for multifiber spectrographs like *Hydra* and *Dohydra*.

The results of our last campaign are shown in Fig. 3. In the right panel of this figure we represent the 400 galaxies for which we have measured the redshifts (six-pointed stars). This plot also includes galaxies with spectroscopy available in the SDSS-DR6 (filled pentagons). The histograms shown in the left panel of Fig. 4 describe the redshift distribution of galaxies measured in the AF2-WYFFOS survey. There are two prominent peaks, at $z \approx 0.07$ and $z \approx 0.11$ respectively. For comparison, we also represent the histogram of redshift distribution in the cluster A2065 (centre panel), and in an intercluster region of the CrB-SC located apart from the positions of the CMB decrement and any known cluster (right panel). In Fig. 5 (left) we can see the redshift histograms of galaxies within circles of different radii and centred at CrB-H. The double-peaked nature of the distribution is obvious for radii greater than 10 arcmin. This could be indicative of the presence of two major structures at $z \approx 0.07$ and $z \approx 0.11$, with a possible interconnection, as suggested by the noticeable excess of galaxies at intermediate redshifts. The contribution of galaxies at $z \approx 0.11$ is predominant for $r \leq 25$ arcmin. For comparison, we also represent (right) the redshift distribution, obtained from the SDSS-DR6 spectroscopic catalogue, of the galaxy cluster A2069, which is at $z \sim 0.11$. As we can see, this redshift distribution as a function of radius is similar to the second peak at $z \approx 0.11$ of the CrB-H histogram. Therefore, we conclude that the galaxy excess at $z \approx 0.11$ in the position of CrB-H is consistent with the presence of an unknown galaxy cluster.

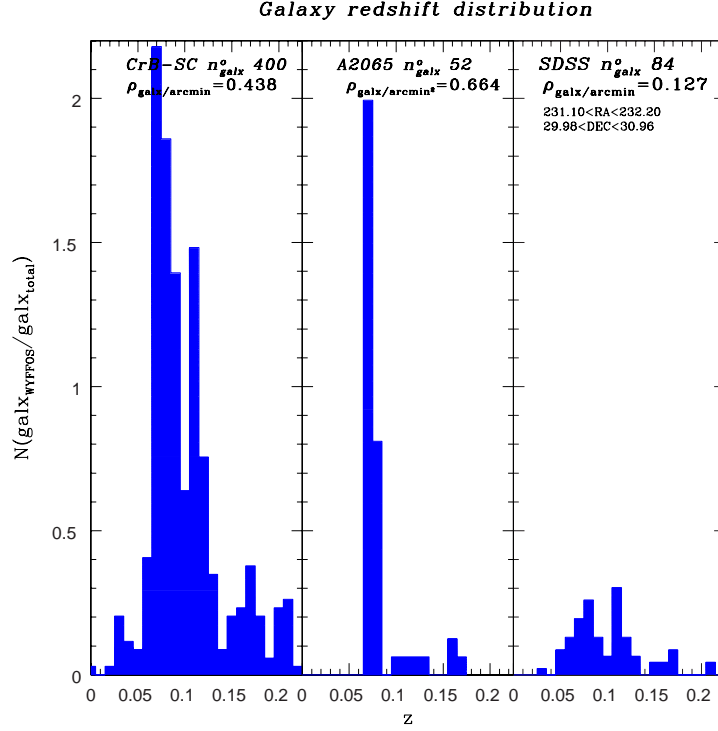


Fig. 4 Redshift histograms of the galaxies at the positions of the CrB-H spot (left), the A2065 galaxy cluster (centre), and a SDSS CrB-SC control region at $231.10^{\circ} \leq \text{R.A.} \leq 232.20^{\circ}$ and $29.98^{\circ} \leq \text{Dec.} \leq 30.98^{\circ}$

3 Conclusions

We have presented a study of the galaxy population in the region of CrB-H, a CMB cold spot found by the VSA at 33 GHz in the CrB-SC, that could be indicative of the presence of diffuse intergalactic warm/hot gas. We have used the SDSS data to analyse the density and photometric properties of the galaxies located around this position. The density of galaxies within the spot is intermediate between that of galaxy clusters and randomly selected all-sky areas (we indeed found only 1 – 2% of such areas with densities larger than that of CrB-H). The galaxy distribution is homogeneous on the sky, and does not show any especial radial dependence. This population of galaxies could be tracing the warm/hot gas that produces the CMB decrement.

We conducted spectroscopic observations of a sample of these galaxies and found that they are located mostly in a redshift interval extending from $z \approx 0.055$ to $z \approx 0.095$. This suggests the presence of a filamentary structure with a length of tens

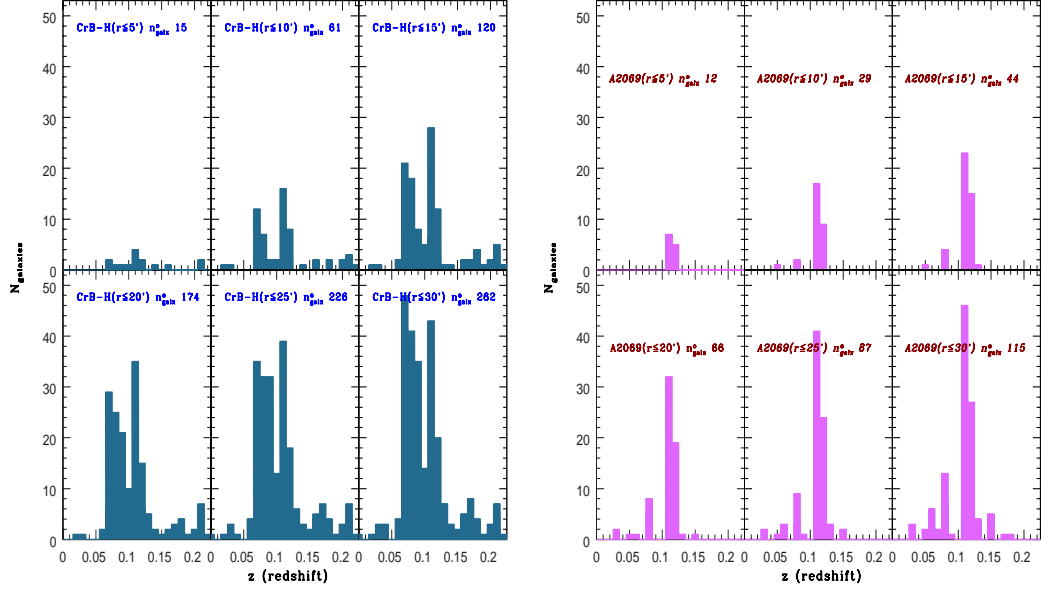


Fig. 5 **Left:** Redshift histograms of galaxies within circles of radii from 5 to 30 arcmin and centred at the position of the CrB-H spot. These redshifts have been obtained from the WHT observations. Two different peaks are found at $z \approx 0.07$ (the redshift of the CrB-SC) and $z \approx 0.11$. **Right:** Redshift histograms of galaxies within circles of radii from 5 to 30 arcmin and centred at the position of the galaxy cluster A2069. In this case the redshifts have been obtained from the SDSS-DR6 spectroscopic catalogue.

of Mpc along the line of sight. We also found a significant excess of galaxies at $z \sim 0.11$, which might point to the presence of a previously unknown cluster at this redshift. The existence of warm/hot gas in the region could be related to the high number of galaxies that we found with strong Balmer emission lines in their spectra.

References

1. Génova-Santos, R., et al. 2005, *MNRAS*, 363, 79
2. Genova-Santos, R., et al. 2008, arXiv:0804.0199
3. Shane, C. D., & Wirtanen, C. A. 1954, *AJ*, 59, 285
4. Abell, G. O. 1958, *ApJs*, 3, 211
5. Postman, M., Geller, M. J., & Huchra, J. P. 1988, *AJ*, 95, 267
6. Small, T. A., Sargent, W. L. W., & Hamilton, D. 1997, *ApJs*, 111, 1
7. Einasto, M., Einasto, J., Tago, E., Müller, V., & Andernach, H. 2001, *AJ*, 122, 2222
8. Small, T. A., Ma, C.-P., Sargent, W. L. W., & Hamilton, D. 1998, *ApJ*, 492, 45
9. Dickinson, C., et al. 2004, *MNRAS*, 353, 732
10. Battistelli, E. S., et al. 2006, *ApJ*, 645, 826 *MNRAS*, 365, 539
11. Lancaster, K., et al. 2005, *MNRAS* 359, 16